Experimental and Computational Ice Shapes and Resulting Drag Increase for a NACA 0012 Airfoil

Jaiwon Shin and Thomas H. Bond
Aerospace Engineer
NASA Lewis Research Center
Cleveland, Ohio

Abstract

Tests were conducted in the Icing Research Tunnel (IRT) at the NASA Lewis Research Center to document the repeatability of the ice shape over the range of temperatures varying from -15°F to 28°F. Measurements of drag increase due to the ice accretion were also made. The ice shape and drag coefficient data, with varying total temperatures at two different airspeeds, were compared with the computational predictions. The calculations were made with the 2D LEWICE/IBL code which is a combined code of LEWICE and the interactive boundary layer method developed for iced airfoils. Comparisons show good agreement with the experimental data in ice shapes. The calculations show the ability of the code to predict drag increases as the ice shape changes from a rime shape to a glaze shape.

Introduction

Over the past few years, the Icing Research Tunnel (IRT) at the NASA Lewis Research Center has gone through several rehabilitations which have improved its capabilities in simulating real icing conditions. Some of the improvements include a new and more powerful fan motor, a new spray bar system, a new digital control system, and various improvements to the IRT structure. As a result, the IRT can now provide more accurate control of the airspeed and temperature, more uniform clouds covering a larger cross-section of the test section, and lower liquid water content.

Although various test programs have been conducted in the IRT with the improved capabilities, there has not been a comprehensive test program to document the repeatability of the data obtained in the IRT. Tests were conducted to address the repeatability issue during the months of June and July of 1991. The test matrix was focused to document the repeatability of the ice shape over a range of air temperatures. During the tests, the drag increase due to the ice accretion was also measured. This test program also provided a new database for code validation work.

The LEWICE code, which is being used by industry and government to predict two-dimensional ice accretions, was combined with the interactive boundary layer method to also predict the resulting aerodynamic penalties[1] (This combined code is referred to as the 2D LEWICE/IBL code.). An initial validation study[2] was made last year, in which the code predictions were compared with the experimental results of Olsen, et al.[3] The results showed good agreement between the experiment and the calculation for both ice shapes and the resulting drag. More comparisons of calculations with experimental data were recommended and the recent repeatability test provided a needed data set.

In this paper, comparisons of measured ice shapes and predicted ice shapes are presented for a range of temperatures with two different airspeeds and liquid water contents. Resulting drag increase is also compared between the experiment and the calculation.

Nomenclature

A	damping-length constant
c	airfoil chord
C_d	drag coefficient
k_s	equivalent sand-grain roughness
k_s^+	dimensionless sand-grain roughness
L	mixing length
T_T	total air temperature
T_s	static air temperature
u_τ	friction velocity
V_∞	airspeed
x	surface coordinate
y	coordinate perpendicular to x
y^+	a Reynolds number, $y\, u_\tau / \nu$
κ	universal constant, also used as a sweep parameter
ν	kinematic viscosity

Description of the Experiment

Icing Research Tunnel

The NASA Lewis Icing Research Tunnel is a closed-loop refrigerated wind tunnel. Its test section is 6 ft. high, 9 ft. wide, and 20 ft. long. A 5000 hp fan provides airspeeds up to 300 mph in the test section. The 21,000 ton capacity refrigeration can control the total temperature from -40°F to 30°F. The spray nozzles provide droplet sizes from approximately 10 to 40 μm median volume droplet diameters (MVD) with liquid water contents (LWC) ranging from 0.2 to 3.0 g/m^3. A schematic of the tunnel, shop, and control room is shown in Fig.1. A detailed description of the IRT can be found in reference 4.

Test Model

The test model was a 6 ft. span, 21 in. chord NACA 0012 airfoil with a fiberglass skin. The model was mounted vertically in the center of the test section. During all icing runs, the model was set at 4° of angle of attack. The model installed in the test section is shown in Fig.2.

Test Conditions

The test points used to make comparisons with the calculation in this paper were selected from the larger test matrix which is fully described in reference 5.

The test conditions given in Table 1 can be grouped into two: 1) low airspeed and high LWC, and 2) high airspeed and low LWC. Water droplet size was held constant for both groups. Airspeed, LWC, and spray time were selected so that both groups would have the same water intercept (i.e. airspeed × LWC × spray time = constant). Temperatures were selected to cover glaze, rime, and transition regimes.

Test Methods

A typical test procedure for icing runs is listed below.

1. The model angle of attack was set.
2. The target airspeed and total temperature were set.
3. The spray system was adjusted to the desired MVD and LWC.
4. The spray system was turned on for the desired spray time.
5. The tunnel was brought down to idle and the frost beyond the ice accretion was removed.
6. The wake survey was traversed across the airfoil wake with the tunnel at the target airspeed.
7. The tunnel was brought down to idle again for ice shape tracings and photographs.
8. The airfoil was then cleaned and the next data point was performed.

Drag Wake Survey

The section drag at the mid-span of the airfoil was calculated from total pressure profiles measured by a pitot-static wake survey probe. The wake survey probe was positioned two chord lengths downstream of the airfoil as shown in Fig.2. The wake surveys were made only when the spray cloud was turned off. During sprays, the probe was kept behind a shield to prevent any ice accretion on the tip of the probe. The wake probe was mounted on an automatic traverse system, and the traversing speed was adjustable.

Description of 2D LEWICE/IBL

LEWICE is a two-dimensional ice accretion code which has a Hess-Smith two-dimensional panel code for a flow calculation, a droplet trajectory and impingement calculation code, and an icing thermodynamic code. Detailed description of the code can be found in reference 6.

Several modifications have been made to the original LEWICE code to add a capability of calculating aerodynamic characteristics by making use of the interactive boundary layer method developed by Cebeci, et al[7]. Along with this new capability, a modification was made to the original LEWICE so that the calculation can be made in a user interaction-free environment. This was achieved by using a smoothing routine[1] to avoid the occurrence of multiple stagnation points caused by the formation of irregular ice surfaces on the ice shape.

During the development of the 2D LEWICE/IBL code, a turbulence model has also been developed to deal with surface roughness such as that associated with ice. This was done by modifying the mixing length and wall-damping expression of the Cebeci-Smith model, that is

$$L = \kappa(y + \Delta y)\{1 - exp[-(y + \Delta y)/A]\} \qquad (1)$$

where Δy is a function of an equivalent sand grain roughness k_s. In terms of dimensionless quantities, with $k_s^+ = k_s u_\tau / \nu$ and $\Delta y^+ = \Delta y\, u_\tau / \nu$

$$\Delta y^+ = \begin{cases} 0.9[\sqrt{k_s^+} - k_s^+ exp(-k_s^+/6)] & 5 < k_s^+ \le 70 \\ 0.7(k_s^+)^{0.58} & 70 \le k_s^+ \le 2000 \end{cases} \qquad (2)$$

The equivalent sand grain roughness for ice is determined from the expressions used in the original LEWICE code.

The heat transfer model used in the LEWICE code makes use of an equivalent sand grain roughness, k_s, expressed as a function of LWC, static air temperature (T_s), and airspeed (V_∞).

The original expression for k_s is in the following form with c denoting the airfoil chord and $(k_s/c)_{base} = 0.001177$

$$k_s = [\frac{k_s/c}{(k_s/c)_{base}}]_{LWC} \cdot [\frac{k_s/c}{(k_s/c)_{base}}]_{T_s} \cdot [\frac{k_s/c}{(k_s/c)_{base}}]_{V_\infty} \cdot (\frac{k_s}{c})_{base} \cdot c \qquad (3)$$

where each sand grain roughness parameter is given by

$$[\frac{k_s/c}{(k_s/c)_{base}}]_{LWC} = 0.5714 + 0.2457(LWC) + 1.2571(LWC)^2 \qquad (4)$$

$$[\frac{k_s/c}{(k_s/c)_{base}}]_{T_s} = 0.047\, T_s - 11.27 \qquad (5)$$

$$[\frac{k_s/c}{(k_s/c)_{base}}]_{V_\infty} = 0.4286 + 0.0044139\, V_\infty \qquad (6)$$

Recent numerical studies conducted by Shin, et al.[2] showed that the equivalent sand grain roughness did not depend on airspeed, but did depend on the median volume diameter (MVD) of the water droplets. As a result, equation (3) is modified, as given by equation (7).

$$k_s = 0.6839\, [\frac{k_s/c}{(k_s/c)_{base}}]_{LWC} \cdot [\frac{k_s/c}{(k_s/c)_{base}}]_{T_s} \cdot [\frac{k_s/c}{(k_s/c)_{base}}]_{MVD} \cdot (\frac{k_s}{c})_{base} \cdot c \qquad (7)$$

where

$$[\frac{k_s/c}{(k_s/c)_{base}}]_{MVD} = \begin{cases} 1 & MVD \le 20 \\ 1.667 - 0.0333\, MVD & MVD > 20 \end{cases} \qquad (8)$$

The interactive boundary layer method then uses a roughness parameter as given in equation (9) over the predicted iced surface.

$$(k_s)_{IBL} = 2(k_s)_{equation\ (7)} \qquad (9)$$

Present studies as well as those conducted in reference 2 showed that drag coefficients calculated with the roughness parameter by the above method were much lower than measured drag coefficients, especially for rime ice shapes. Numerical studies were conducted to investigate the effect of the extent of the iced airfoil surface on drag. In the original version of the 2D LEWICE/IBL code, roughness is only applied over the surface of the ice. The code was modified to allow for roughness on both the ice and the airfoil surface downstream of the ice. The results showed that agreement between calculated and measured drag coefficients for rime ice shapes became much better by extending the range of the roughness on the airfoil surface and placing a lower limit of $k_s/c = 0.002$ on the equivalent sand grain roughness, which otherwise would become very small for rime ice. The extent of the iced airfoil surface which resulted in the best agreement with the experimental drag coefficients for rime ice shapes was found to be 50 percent of the airfoil chord, and this extent was used in all drag calculations presented in this paper.

Results and Discussion

This section contains a discussion of the quality of the experimental data, and discussions of the ice shape comparison and the iced airfoil drag comparison.

Quality of Experimental Data

Dry airfoil drag results - Section drag was measured with the clean airfoil under the dry condition and the results are compared with the published data[3,8,9] as shown in Fig.3. The data of Abbott and Doenhoff[8] was taken in the Low Turbulence Pressure Tunnel (LTPT) at the NASA Langley Research Center. The data of Olsen, et al.[3] and the data of Blaha and Evanich[9] were taken in the IRT.

The difference between the data from the LTPT and the IRT can occur for several reasons: differences in wake survey method, tunnel turbulence level, and model condition. The LTPT tests used a wake rake while the IRT tests used a traversing probe. The LTPT had the freestream turbulence intensity of the order of a few hundredths of 1 percent. The freestream turbulence intensity in the IRT is about 0.5 percent. The difference in the surface finish of a model can also have an effect on drag.

The current IRT drag data is higher than the previous IRT data. All three tests used the wake survey method and the airfoils had the same chord length. This kind of difference in drag data can come from differences in the wake survey location and model condition. The wake survey probe was located at one chord length behind the model for Blaha's test while it was located at two chord lengths behind the model for Olsen's test and the current test. The leading edge and the trailing edge part of the current model were joined at the maximum thickness location (30 percent of the chord) while the model used in both reference 3 and 9 was the same one-piece airfoil.

According to the experimental results of Gregory and O'Reilly[10] shown in Fig.4, transition occurs at around 40 percent chord at 0° of angle of attack for an NACA 0012 airfoil at a Reynolds number of 3 million. The transition location moves upstream very rapidly as the angle of attack increases. A small step at the joint in the current model may have acted as a trip at low angles of attack causing an early transition to turbulent boundary layer. At higher angles of attack, the step may have acted as an additional roughness source in the turbulent boundary layer, which increased drag.

Drag associated with an iced airfoil is normally dominated by the pressure drag due to a large separation caused by a pressure spike at the upper horn. At 4° of angle of attack, where all the icing runs were made, an increase of the friction drag by the step of the current model is believed to have a minimal effect on icing drag data.

Repeatability of dry airfoil drag measurements - Dry runs were made prior to each icing run. Each icing run was repeated at least twice, which resulted in more than 28 dry airfoil drag measurements at a 4° angle of attack. The percent variation was calculated in the same way as Olsen[3] by taking the standard deviation and dividing it by the average. The average C_d value at a 4° angle of attack was 0.01068. The percent variation was 7.1 percent of the average value. The percent variation reported by Olsen was 7.7 percent.

Repeatability of the ice shapes and resulting drag - Each data point was repeated at least twice to ensure repeatability of the ice shape and drag measurement. Ice shapes and measured drag coefficients of three repeat runs for typical glaze ice (22°F) and rime ice (-15°F) cases at two airspeeds are shown in Figs. 5 and 6.

At all four conditions, the ice shape repeats well and the variation of the drag coefficient is within the percent variation of the measurement. The larger percent variation is seen with glaze ice, however the variation is much smaller than that reported in Olsen[3].

Comparison Between Calculated and Measured Ice Shapes

Ice shapes were computed with the 2D LEWICE/IBL code for the icing conditions shown in Table 1. Since the code runs without any user interactions, the only variable which can influence the ice shape for a given icing condition is the time step. Previous investigation[2] suggested that the use of 1 minute time interval resulted in the best agreement with the experimental ice shapes.

To ensure the above finding still holds true, the effect of time step was investigated with all icing conditions at the airspeed of 150 mph. Four different time intervals, 0.5, 1, 2, and 6 minutes, were used. Figure 7 shows the results for a glaze ice, a rime ice, and a transition case. The use of a longer time interval results in more ice accretion as seen in all cases. Based on the comparison with the experimental data, 1 min time step was chosen for all the calculations.

Figure 8 shows calculated and measured ice shapes at various temperatures. The experimental ice shape changes from white, opaque rime ice to slushy, clear glaze ice with increased temperature. Airspeed was set at 150 mph. Experimental ice shapes were taken at the mid-span of the model where the wake survey was made. The agreement between calculated and measured ice shapes is good, particularly for rime ice cases. Icing limits are predicted well for the temperatures below 18°F. At warmer temperatures, the calculation predicted more run back which resulted in more ice accretion beyond the experimental icing limits. The direction of horn growth is predicted reasonably well, but in general the size of the predicted ice shape is larger than the measured shape.

Figure 9 shows ice shape comparison as a function of temperature at the airspeed of 230 mph. Comparisons show similar results as the lower speed cases. Good agreement is shown at all temperatures except at 28°F where an overprediction of upper horn is seen.

Comparison between Calculated and Measured Drag

Calculated drag coefficients were compared with measured drag coefficients for the ice shapes shown in Figs.8 and 9. With each icing run, the wake survey was made twice: one made while the probe traversed away from the shield, and the other made while the probe traversed back to the shield. Each measured drag coefficient in Table 2 is the averaged value of the two measurements at each icing run. Calculated drag coefficients are also included in Table 2 for comparisons.

Results in Table 2 are plotted in Figs.10 and 11. For both airspeeds, the experimental data show almost constant measured drag coefficients up to around 12°F and a sharp increase toward near freezing temperatures as the ice shape changes to glaze ice. For V_∞ = 150 mph, calculated drag coefficients agree very well with measured drag coefficients up to 12°F and begin to rise sharply at around 18°F. While calculated drag coefficients reach a peak at around 22°F and begin to decrease, measured drag coefficients continue to rise and reach a peak at around 28°F. For V_∞=230 mph, however, the calculated results does a good job of following the trend in measured values.

Concluding Remarks

The ice shape and drag coefficient results of the experimental program conducted in the IRT were compared with the predictions using the 2D LEWICE/IBL code. Experimental data provided validation data to further calibrate the code with various icing parameters such as the temperature, airspeed, and LWC. Good agreement in the ice shape was shown for the rime ice. The agreement deteriorated for the glaze ice, although the direction of the horn growth was generally predicted well. Deterioration in ice shape prediction for glaze ice is a typical characteristic shown with the original LEWICE code. The ice shape comparison results indicate that the modifications made to the original LEWICE code in the process of combining it with the interactive boundary layer method work well.

The results of the drag comparison study show the ability of the code to predict the sharp drag increase displayed by the experimental data as the ice shape changes from rime to glaze. The adjustment made by extending the roughness beyond the icing limit on the airfoil allows the calculated drag values to agree well with experimental data. More studies are needed to better estimate the extent of icing on the airfoil surface.

The big strength of the 2D LEWICE/IBL code is the economy of the computing time. A typical computing time (CPU time only) to complete a calculation of 6 or 7 minutes ice accretion and its aerodynamic characteristics was less than 50 seconds on a CRAY X-MP.

More comparison work is needed to check the 2D LEWICE/IBL code for further improvements. The test points of the repeatability test in the IRT were reduced from the original test plan due to the loss of tunnel time. More tests are planned to document the effects of other icing parameters on the ice shape and resulting drag. It is also planned to obtain experimental lift data with iced airfoils for code validation work.

References

1. Cebeci, T., Chen, H.H., and Alemdaroglu, N., "Fortified LEWICE with Viscous Effects," Journal of Aircraft, Vol.28, No.9, pp. 564-571, Sept. 1991.
2. Shin, J., Berkowitz, B., Chen, H.H., and Cebeci, T., "Prediction of Ice Shapes and Their Effect on Airfoil Performance," AIAA-91-0264, 1991.
3. Olsen, W, Shaw, R., and Newton, J., "Ice Shapes and the Resulting Drag Increase for a NACA 0012 Airfoil," NASA TM 83556, 1984.
4. Soeder, R.H. and Andracchio, C.R., "NASA Lewis Icing Research Tunnel User Manual," NASA TM 102319, 1990.
5. Shin, J. and Bond, T, "Results of an Icing Test on a NACA 0012 Airfoil in the NASA Lewis Icing Research Tunnel," AIAA-92-0647, 1992.
6. Ruff, G.A. and Berkowitz, B.M., "Users Manual for the NASA Lewis Ice Accretion Prediction Code (LEWICE)," NASA CR 185129, 1990.
7. Cebeci, T., "Calculation of Flow Over Iced Airfoils," AIAA Journal, Vol.27, No.7, pp.853-861, 1989.
8. Abbott, I.H. and Von Doenhoff, A.E., Theory of Wing Sections, pp. 462-463, Dover Publications, Inc., 1959.
9. Blaha, B.J. and Evanich, P.L., "Pneumatic Boot for Helicopter Rotor Deicing," NASA CP-2170, 1980.
10. Gregory, N. and O'Reilly, C.L., "Low-Speed Aerodynamic Characteristics of NACA 0012 Airfoil Section, Including the Effects of Upper-Surface Roughness Simulating Hoar Frost," NPL AERO Report 1308, 1970.

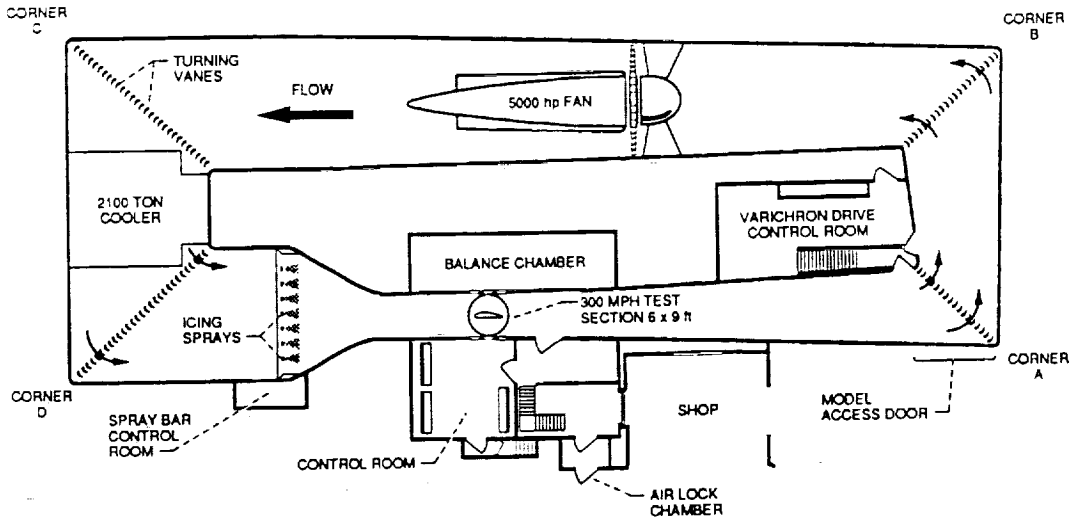

Fig.1. Plan View of IRT, Shop, and Control Room.

Table 1. Test Conditions

AOA (deg.)	Air Speed (mph)	LWC (g/m^3)	MVD (μm)	Total Temperature (^oF)	Ice Accretion Time (min.)
4	150	1.0	20	28	6
4	150	1.0	20	25	6
4	150	1.0	20	22	6
4	150	1.0	20	18	6
4	150	1.0	20	12	6
4	150	1.0	20	1	6
4	150	1.0	20	-15	6
4	230	0.55	20	28	7
4	230	0.55	20	25	7
4	230	0.55	20	22	7
4	230	0.55	20	18	7
4	230	0.55	20	12	7
4	230	0.55	20	1	7
4	230	0.55	20	-15	7

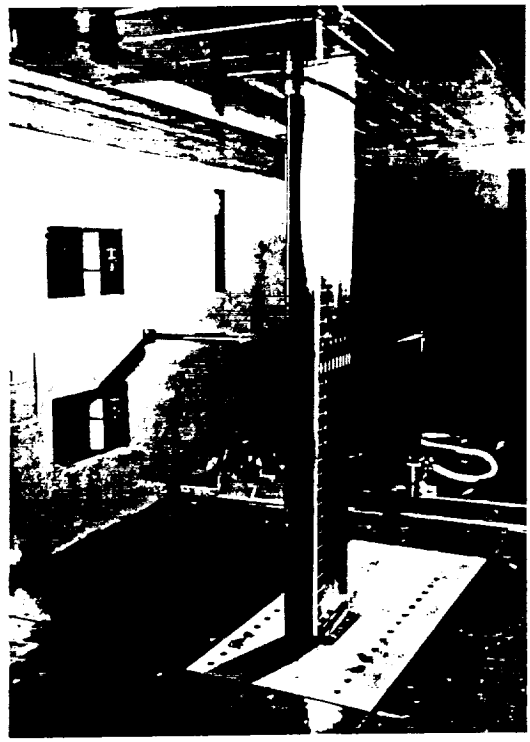

Fig.2. NACA 0012 Airfoil and Wake Survey Probe.

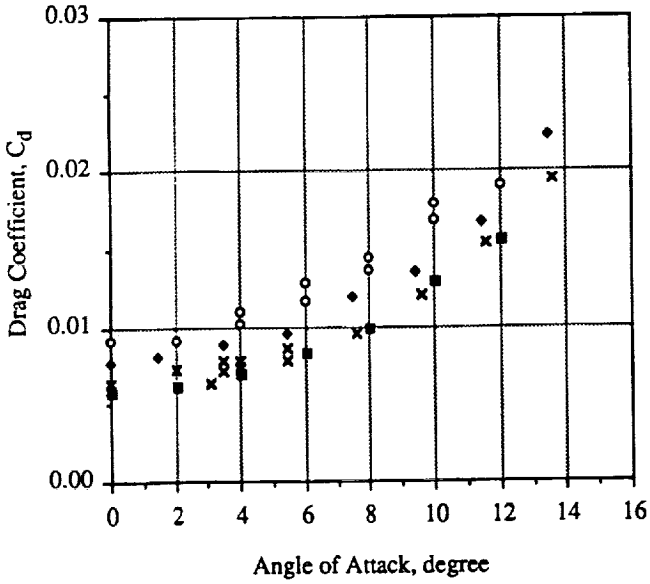

Legend: Facility, Reynolds Number

- IRT, 3 Million
- LTPT, 3 Million (Reference 8)
- IRT, 3 Million (Reference 3)
- IRT, 3 Million (Reference 9)

Fig. 3. Comparison of Measured Clean Airfoil Drag with Published Data for the NACA 0012 Airfoil.

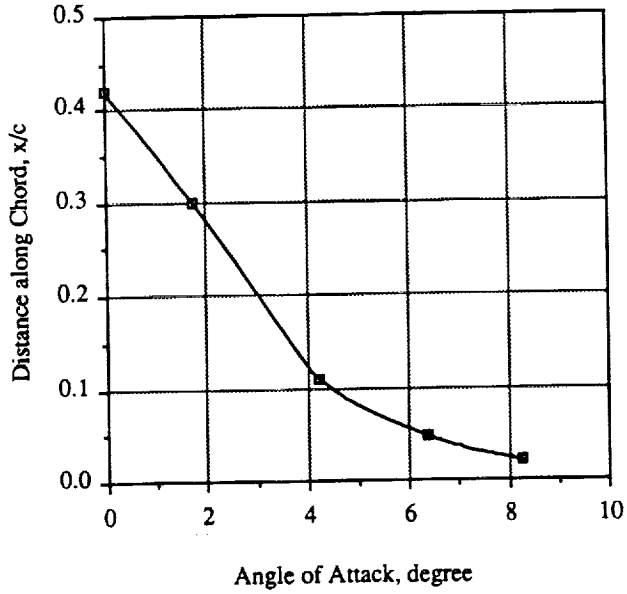

Fig. 4. Transition Locations on the NACA 0012 Airfoil for Re = 2.88×10^6.

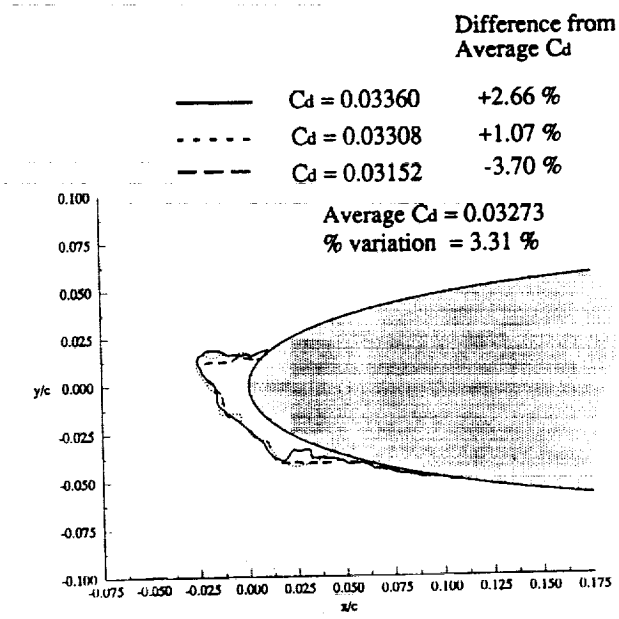

(a) AOA=4°, V_∞=150 mph, T_T=22°F, LWC=1.0g/m^3, MVD=20μm, Accretion Time = 6 min.

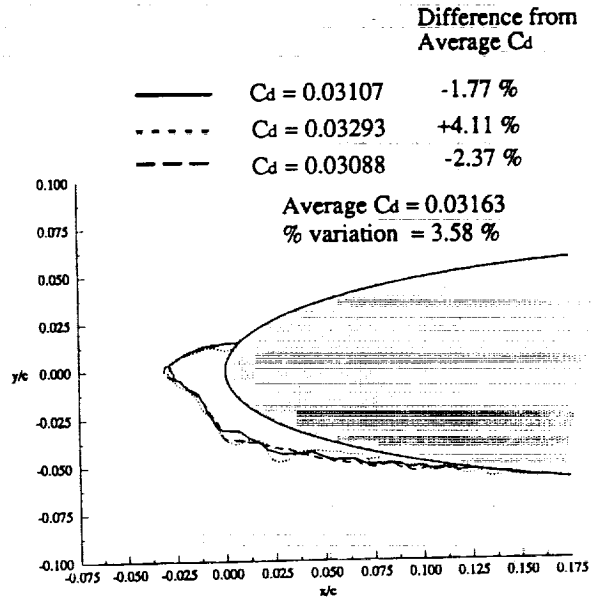

(b) AOA=4°, V_∞=230 mph, T_T=22°F, LWC=0.55g/m^3, MVD=20μm, Accretion Time = 7 min.

Fig. 5. Repeatability of Ice Shape and Drag for Glaze Ice Shapes.

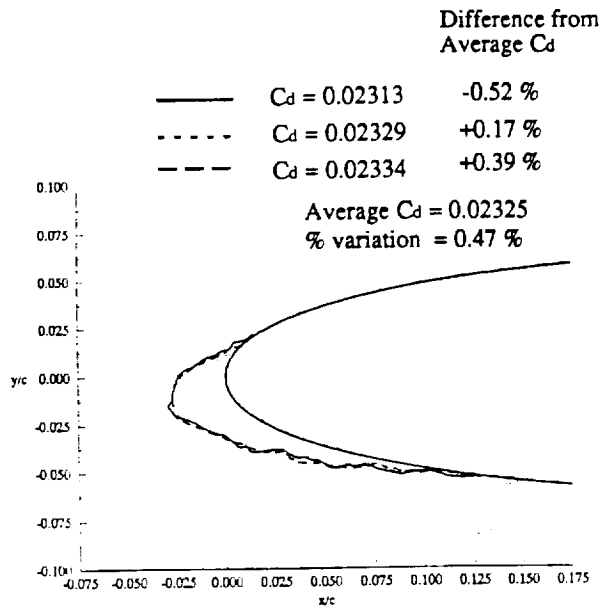

(a) AOA=4°, V_∞=150 mph, T_T=-15°F, LWC=1.0g/m^3, MVD=20μm, Accretion Time = 6 min.

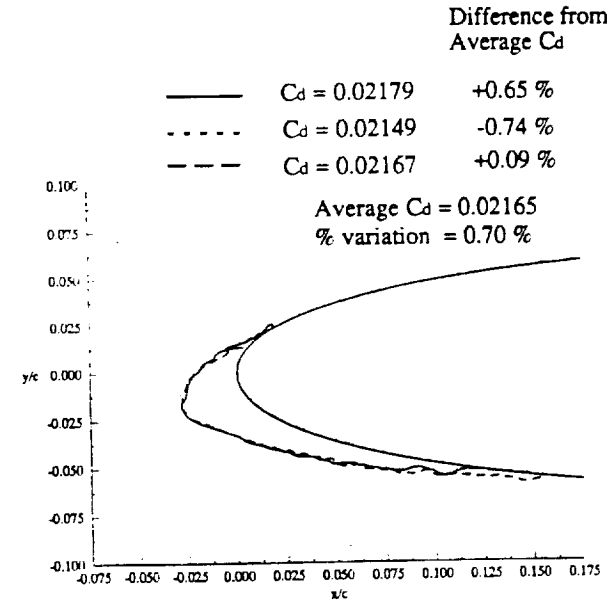

(b) AOA=4°, V_∞=230 mph, T_T=-15°F, LWC=0.55g/m^3, MVD=20μm, Accretion Time = 7 min.

Fig.6. Repeatability of Ice Shape and Drag for Rime Ice Shapes.

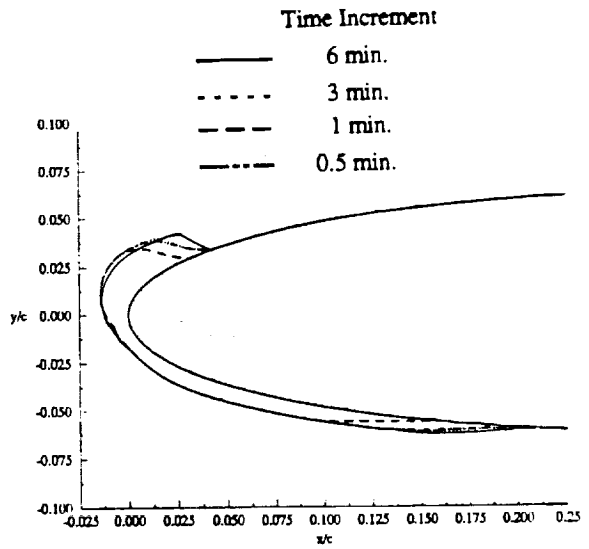

(a) AOA=4°, V_∞=150 mph, T_T=28°F, LWC=1.0g/m^3, MVD=20μm, Accretion Time = 6 min.

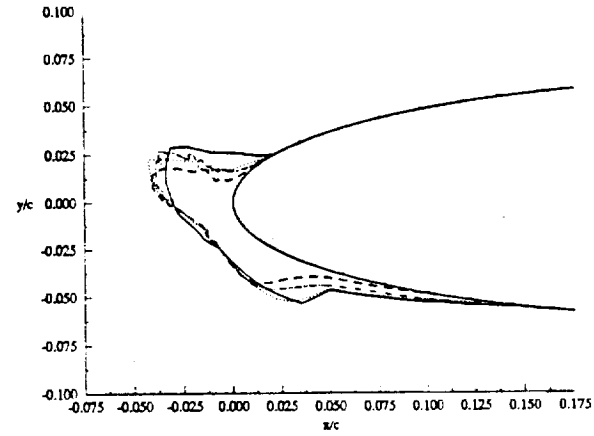

(b) AOA=4°, V_∞=150 mph, T_T=18°F, LWC=1.0g/m^3, MVD=20μm, Accretion Time = 6 min.

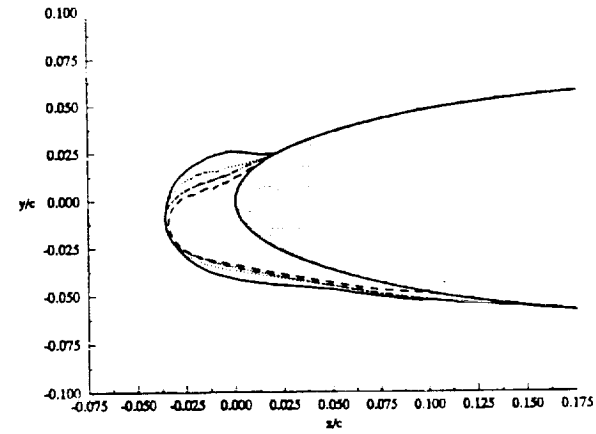

(c) AOA=4°, V_∞=150 mph, T_T=-15°F, LWC=1.0g/m^3, MVD=20μm, Accretion Time = 6 min.

Fig.7. Effect of Computational Time Step on Ice Shape.

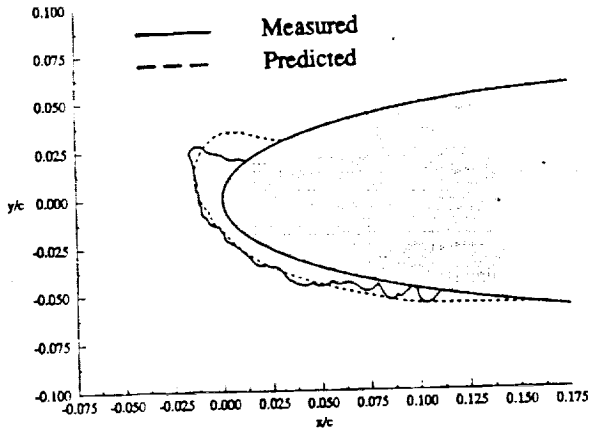

(a) T_T=28°F

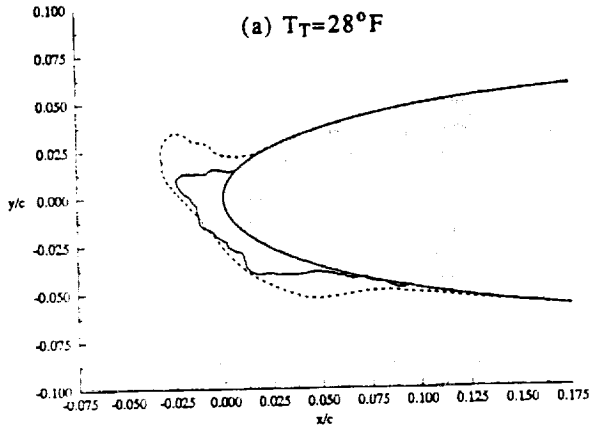

(c) T_T=22°F

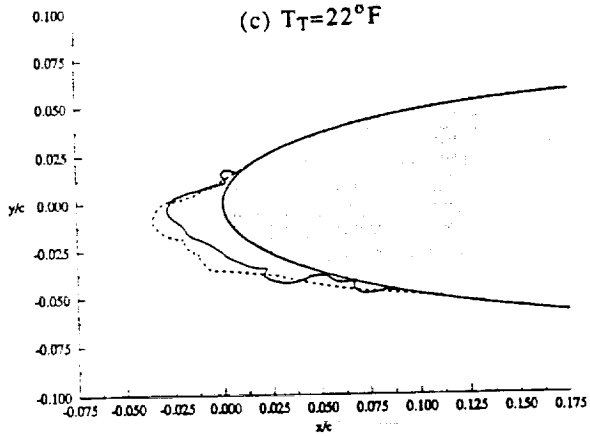

(e) T_T=12°F

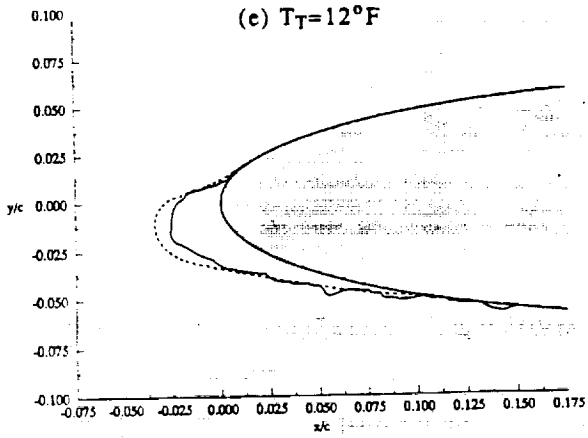

(g) T_T=-15°F

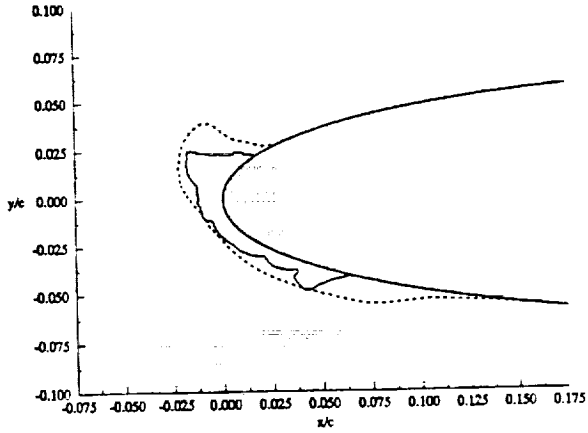

(b) T_T=25°F

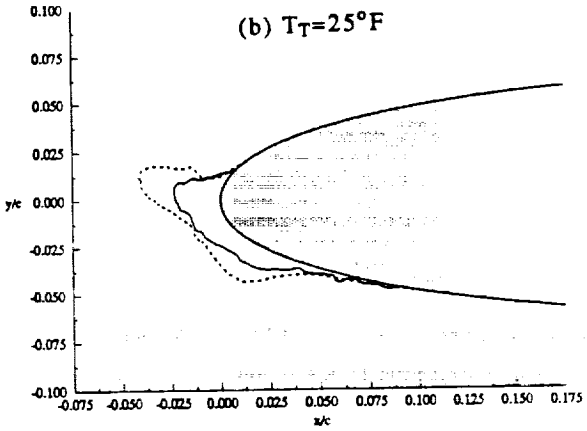

(d) T_T=18°F

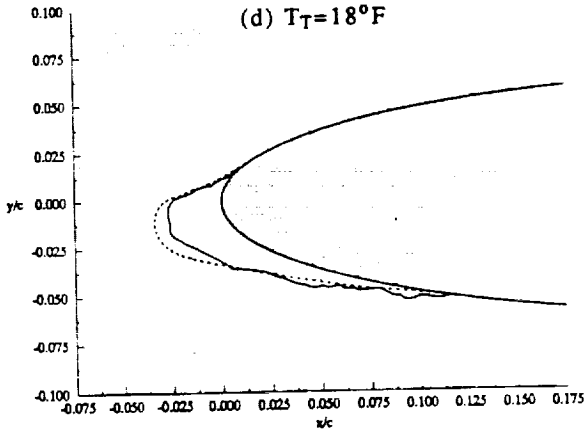

(f) T_T=1°F

Fig. 8. Effect of Total Air Temperature on Ice Shape.

AOA=4°, V_∞=150 mph, LWC=1.0g/m^3, MVD=20μm, Accretion Time = 6 min.

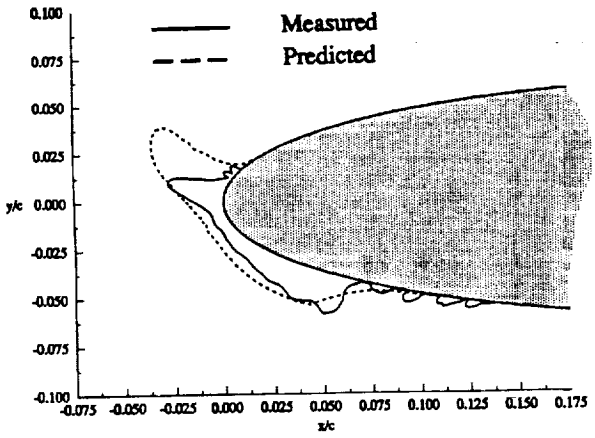

(a) T_T=28°F

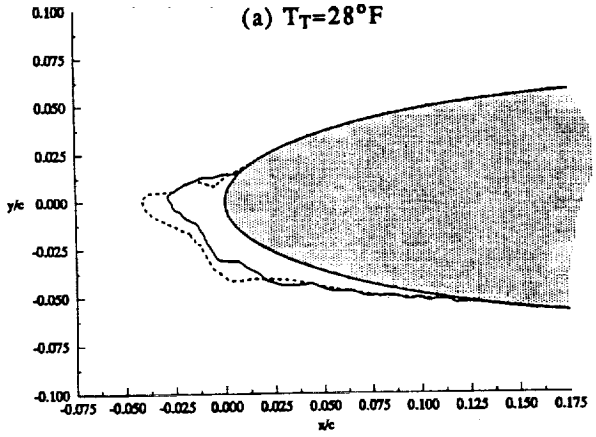

(c) T_T=22°F

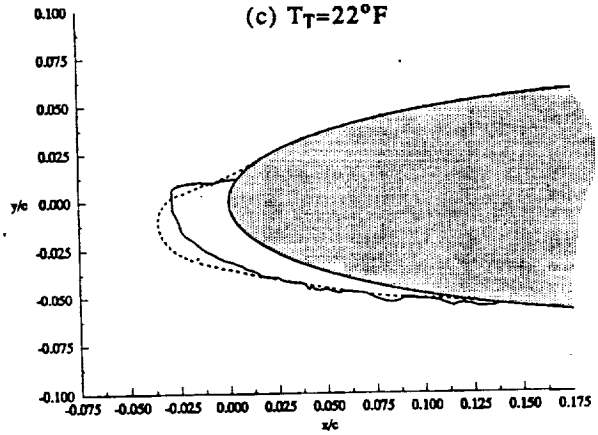

(e) T_T=12°F

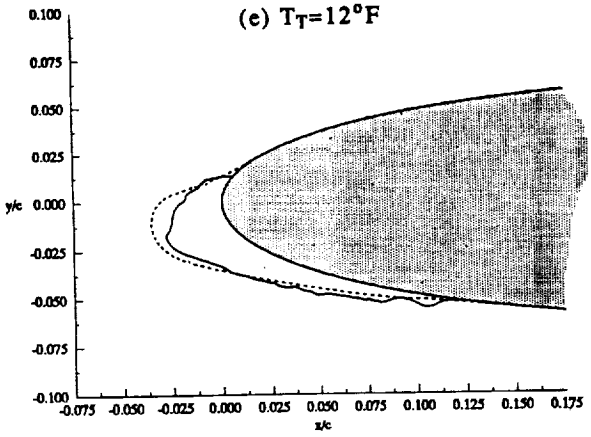

(g) T_T=-15°F

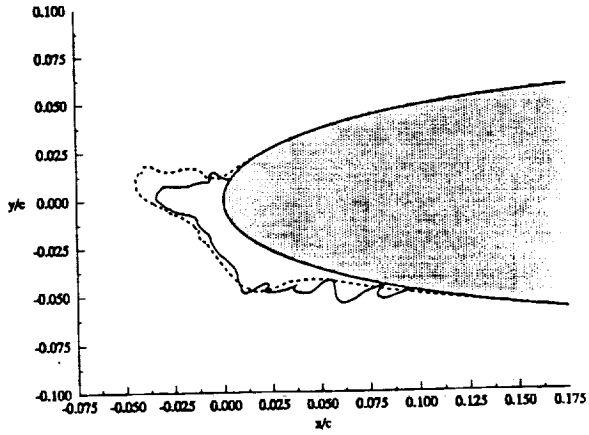

(b) T_T=25°F

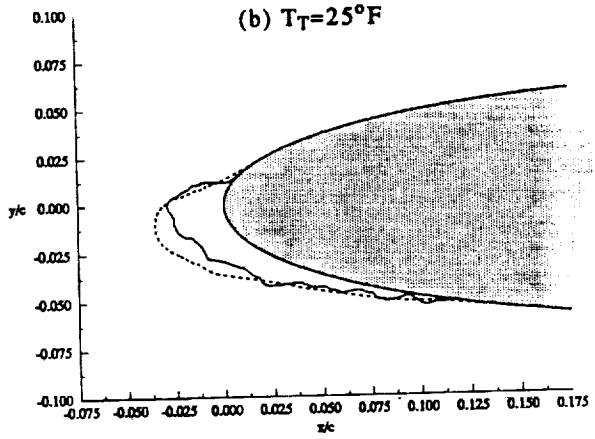

(d) T_T=18°F

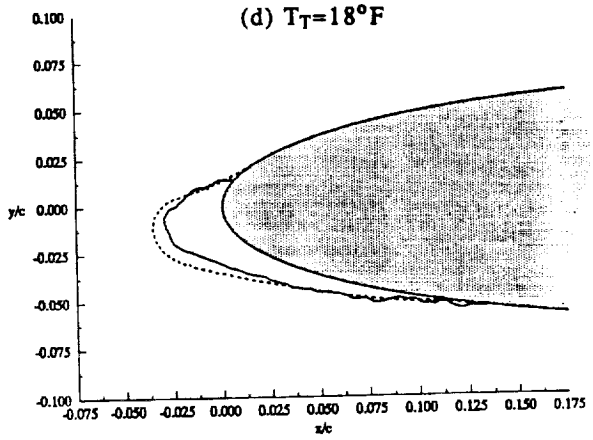

(f) T_T=1°F

Fig.9. Effect of Total Air Temperature on Ice Shape.

AOA=4°, V_∞=230 mph, LWC=0.55g/m^3, MVD=20μm, Accretion Time = 7 min.

Table 2. Effect of Total Air Temperature on Drag Coefficient.

(a) Airspeed=150 mph, LWC=1.0g/m^3, MVD=20μm

Total Temperature (^{o}F)	Experimental Drag Coefficient	Calculated Drag Coefficient
28	0.0578	0.0346
25	0.0540	0.0372
22	0.0315	0.0392
18	0.0271	0.0351
12	0.0229	0.0217
1	0.0229	0.0209
-15	0.0233	0.0202

(b) Airspeed=230 mph, LWC=0.55g/m^3, MVD=20μm

Total Temperature (^{o}F)	Experimental Drag Coefficient	Calculated Drag Coefficient
28	0.0428	0.0470
25	0.0371	0.0294
22	0.0311	0.0202
18	0.0268	0.0195
12	0.0255	0.0195
1	0.0234	0.0195
-15	0.0218	0.0192

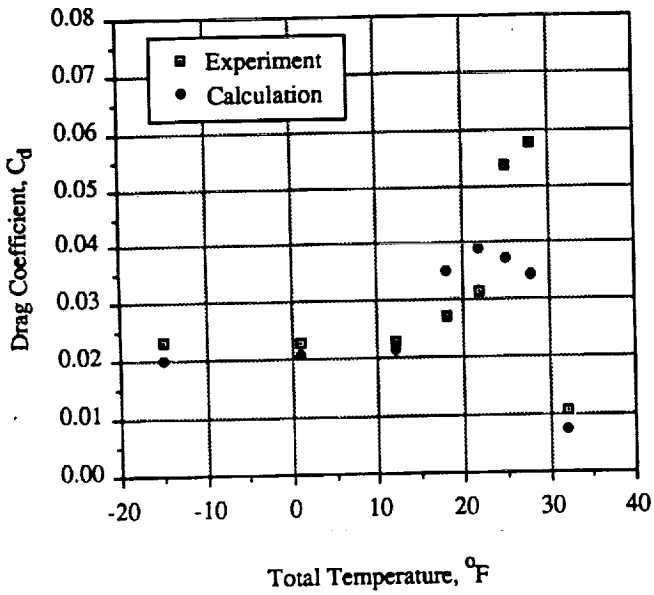

Fig.10. Effect of Total Temperature on Drag (V_∞ =150 mph).

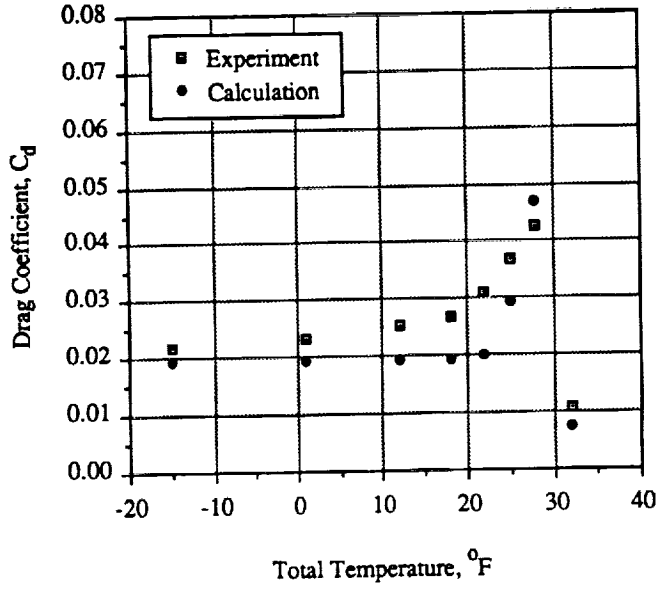

Fig.11. Effect of Total Temperature on Drag (V_∞=230 mph).